Distinct Local Environments of the Pyrene Chromophores in the Covalent Deoxyribonucleic Acid Adducts of 9,10-Epoxy-9,10,11,12-tetrahydrobenzo[*e*]pyrene and 7,8-Dihydroxy-9,10-epoxy-7,8,9,10-tetrahydrobenzo[*a*]pyrene Elucidated by Optically Detected Magnetic Resonance†

Steven M. Lefkowitz‡ and Henry C. Brenner*,§

ABSTRACT: The optically detected magnetic resonance (ODMR) spectra of the covalent DNA adduct of 9,10-epoxy-9,10,11,12-tetrahydrobenzo[*e*]pyrene (BePE) reveal that the excited triplet state chromophore is perturbed by the nucleic acid and that this perturbation is diminished successively by denaturation and enzymatic hydrolysis of the modified DNA, indicating that the adduct resides in an environment with some quasi-intercalative character. In contrast the covalent adduct of 7,8-dihydroxy-9,10-epoxy-7,8,9,10-tetrahydrobenzo[*a*]pyrene shows little ODMR evidence of interaction with the nucleic acid, which, in view of ODMR's sensitivity demonstrated for the BePE adduct, suggests that the chromophore is situated in an environment resembling the bulk solvent. These results demonstrate that ODMR is more sensitive than conventional phosphorescence techniques to interactions between these pyrene-like chromophores and DNA.

Polycyclic aromatic hydrocarbons (PAH)[1] are generally believed to exert their carcinogenic action only after metabolism into chemically reactive species (Harvey & Fu, 1978) and the subsequent binding of these intermediates to cellular DNA (Miller, 1970). The structural characterization of these DNA–carcinogen adducts is of great interest and has as its eventual goal a role in elucidating the evolution of the modified nucleic acid into the final neoplastic transformation. In this paper we exploit the properties of the pyrene-like chromophore's photoexcited triplet state sublevels to probe the binding site structure in the covalent DNA adducts of epoxide derivatives of benzo[*a*]pyrene and benzo[*e*]pyrene, BaPDE and BePE, shown in Figure 1.

BaPDE is the specific in vivo metabolite of benzo[*a*]pyrene that is thought to initiate carcinogenesis by its covalent binding to DNA (Sims et al., 1974; Weinstein et al., 1976; Jeffrey et al., 1977). Since the adduct formed by the incubation of BaPDE with a DNA solution is essentially identical with the in vivo adduct, this in vitro adduct has been the subject of intense study, as the extent of in vitro modification can be made sufficiently high to allow the application of a variety of spectroscopic and biochemical techniques not applicable to the in vivo scantily modified nucleic acid (Weinstein et al., 1978).

Previous work on the BaPDE adduct, relying on adsorption shifts (Geacintov et al., 1982), fluorescence quenching (Prusik et al., 1979) and linear electric dichroism measurements (Geacintov et al., 1978), suggested that the pyrene chromophore is essentially external to the nucleic acid helix and may reside in the DNA minor groove. However, recent studies on DNA fragments of well-defined length using similar techniques (Hogan et al., 1981) and observations on the effects of BaPDE binding to supercoiled DNA (Drinkwater et al., 1978) were interpreted in terms of a model in which the chromophore resides in an intercalative environment.

BePE has not been detected in the metabolism of benzo[*e*]pyrene (Wood et al., 1979; MacLeod et al., 1979) but has been shown to be a potent mutagen in bacteria and mammalian cells (Wood et al., 1979, 1980), presumably exerting this effect by its covalent binding to DNA. In contrast to a body of BaPDE evidence, the chromophore of the BePE–DNA adduct exhibits photophysical properties indicative of considerable interaction with the π-electron clouds of the DNA bases, rather than a freely solvent exposed conformation (Geacintov et al., 1982).

Another important difference between BaPDE and BePE in vitro adduct formation is the degree of conformational specificity of these covalent complexes; while the two bind at analogous bay region carbon positions, BaPDE stereospecifically forms the trans adduct (defined by the relative position of the nucleotide to the nearest hydroxyl group of the adduct) at the exocyclic nitrogen of guanosine (Autrup et al., 1978; Brown et al., 1979), while BePE exhibits both cis and trans adducts, as well as a significant number of adenosine adducts (Kinoshita et al., 1982). The physical measurements mentioned above (Geacintov et al., 1982) also give evidence

† From the Department of Chemistry, New York University, New York, New York 10003. *Received September 9, 1981.* Research support by Grant CA 20851, awarded by the National Cancer Institute, Department of Health and Human Services, to N. E. Geacintov and H.C.B.

‡ Present address: Chemistry Division, Argonne National Laboratory, Argonne, IL 60439.

§ Alfred P. Sloan Fellow.

[1] Abbreviations: BaP, benzo[*a*]pyrene; BaPDE, 7,8-dihydroxy-9,10-epoxy-7,8,9,10-tetrahydrobenzo[*a*]pyrene; BaPT, hydrolysis tetrol of BaPDE; BeP, benzo[*e*]pyrene; BePE, 9,10-epoxy-9,10,11,12-tetrahydrobenzo[*e*]pyrene; BePD, hydrolysis diol of BePE; DNA, deoxyribonucleic acid; EELDOR, electron–electron double resonance; EGB, ethylene glycol–buffer; GHz, gigahertz; HPLC, high-performance liquid chromatography; MHz, megahertz; MIDP, microwave-induced delayed phosphorescence; ODMR, optically detected magnetic resonance; PAH, polycyclic aromatic hydrocarbon.

0006-2960/82/0421-3735$01.25/0

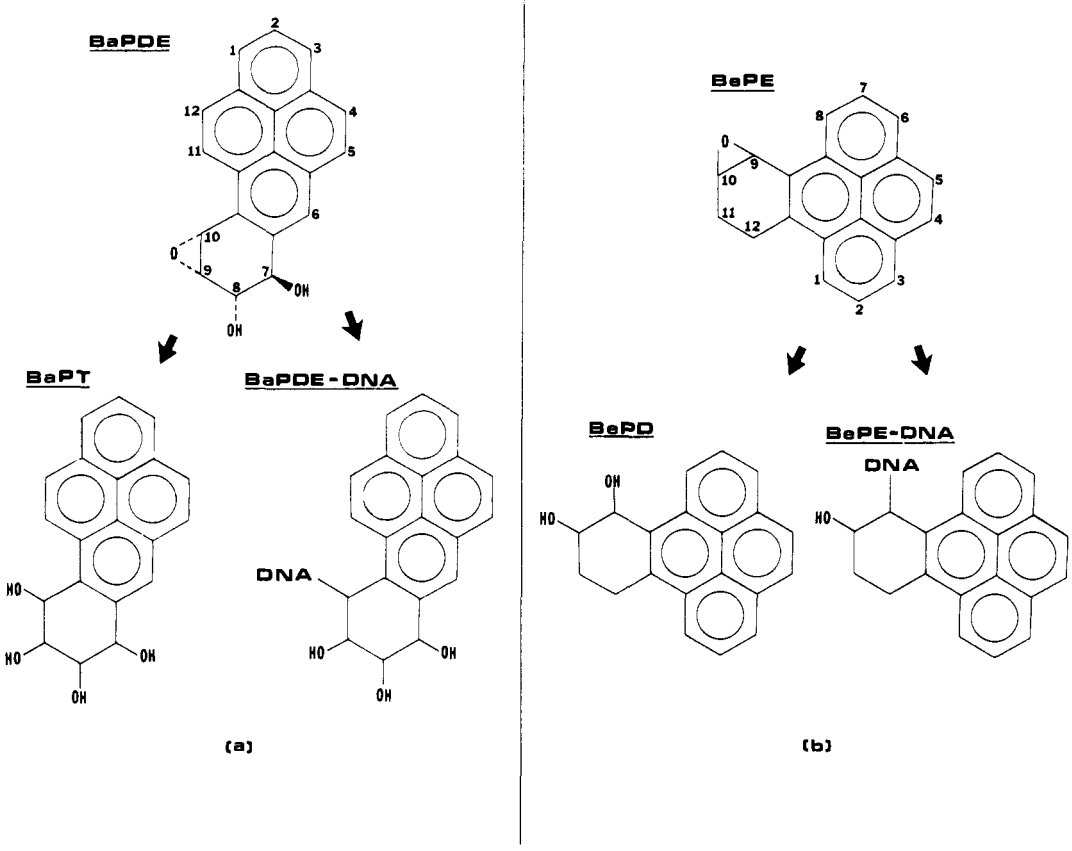

FIGURE 1: Systems studied. (a) BaPDE, 7,8-dihydroxy-9,10-epoxy-7,8,9,10-tetrahydrobenzo[*a*]pyrene; BaPT, hydrolysis tetrol of BaPDE; BaPDE–DNA, covalent DNA adduct of BaPDE. (b) BePE, 9,10-epoxy-9,10,11,12-tetrahydrobenzo[*e*]pyrene; BePD, hydrolysis diol of BePE; BePE–DNA, covalent DNA adduct of BePE.

for considerable conformational heterogeneity in the BePE adduct.

We have studied the DNA adducts of BePE and BaPDE by optically detected magnetic resonance (ODMR) of the photoexcited triplet state of the pyrene-like chromophores in the adducts and model systems. The triplet state consists of three magnetic sublevels whose energy splittings, in the absence of an external magnetic field, arise from the anisotropic interactions of the unpaired electrons' magnetic moments and are characterized by the energy parameters D and E. Figure 2 shows the axes of spin quantization in pyrene and the expected ODMR transitions (Charles et al., 1965). These sublevels possess unique populating and depopulating rates, caused by the different admixtures of singlet character into each sublevel. Hence, large non-Boltzmann population differences between the sublevels will be established at very low temperatures, where spin–lattice relaxation rates are relatively slow.

ODMR exploits the sublevels' cryogenic isolation and unique radiative propensities to determine sublevel splittings by monitoring the total phosphorescence intensity, at some optical wavelength and band-pass, while irradiating the sample with swept frequency micowaves. When a resonance between a pair of sublevels is achieved, the populations are redistributed, leading to a change in the phosphorescence intensity (Kwiram, 1972). Sublevel kinetics are determined by analyzing the response of the phosphorescence to pulsed resonant microwave radiation. Details of both types of measurements are given under Materials and Methods.

Since both the sublevel energy splittings and kinetic differentiation are very sensitive to the symmetry of the excited chromophore, we expect them to reflect any environmentally induced distortions of the unpaired electron density. Earlier ODMR studies yielded preliminary results, suggesting that the pyrene chromophore of the BePE–DNA adduct exhibits a substantial nucleic acid induced perturbation (Lefkowitz & Brenner, 1981), while the BaPDE adduct shows little evidence of interaction with DNA (Lefkowitz et al., 1979). In this paper we consolidate and amplify those studies and present evidence identifying the primary source of ODMR perturbation in the BePE adduct as the double-helical structure of DNA, indicative of some intercalative-like environment for this chromophore, while the BaPDE adduct's ODMR properties closely resemble those expected for the chromophore in

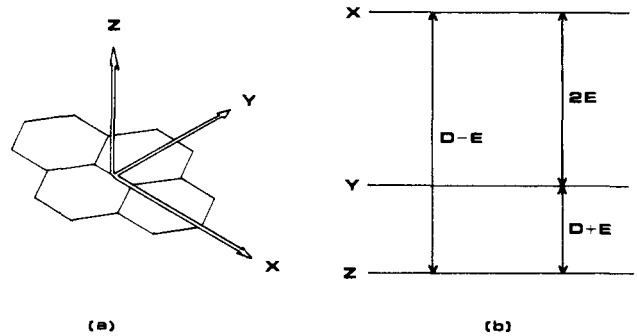

FIGURE 2: Pyrene triplet sublevels. (a) Axes of triplet spin quantization. (b) Sublevel splittings and ODMR transitions.

the bulk solvent, suggesting little interaction with the tertiary DNA structure.

Materials and Methods

Sample Preparation. BaPDE and BePE were kindly provided by Dr. Ronald G. Harvey of the University of Chicago. Calf thymus DNA was purchased from Worthington Chemicals. Preparations of the DNA adducts of BaPDE and BePE in 5 mM cacodylate buffer (pH 7.0) and the separation of the unreacted or hydrolyzed oxides have been described (Prusik et al., 1979) and yielded modification extents of 1–5 adducts per 1000 nucleotides, in DNA solutions ca. 0.001 M in phosphate. Heat-denatured samples were prepared by heating the modified DNA solutions to 100 °C for ca. 20 min and immersing these in an ice–water bath. The denatured samples were extracted with water-saturated ether, with the washes showing no detectable pyrene-like absorption, indicating that the denaturation procedure had not disrupted any adduct-DNA covalent linkages.

The carcinogen-modified deoxyribonucleosides, obtained from the enzymatic hydrolysis of the DNA adducts of BaPDE and BePE, were graciously supplied by Dr. Alan Jeffrey. These unseparated digests were checked by analytical HPLC, with the BaPDE adduct showing a single product and the BePE adduct several, as described earlier in this paper (Kinoshita et al., 1982). All spectroscopic analyses performed here utilized the unseparated digests.

BePE and BaPDE were acid hydrolyzed into the respective BeP diol (BePD) and BaP tetrol (BaPT) (Prusik et al., 1979), both shown in Figure 1. The solvents used were purified, and the pyridine was dried, by standard techniques (Gordon & Ford, 1972). All samples, except for BaPT and BePD, were studied in a 1:1 (v/v) ethylene glycol–buffer solvent system (EGB), which yielded an optical quality glass upon quick freezing by immersion in liquid nitrogen, since samples prepared in pure buffer yielded no detectable ODMR signals. Although the addition of ethylene glycol is known to induce alterations of the conformation of DNA, relative to the pure buffer solvent (Green & Mahler, 1968; Nelson & Johnson, 1970), it is well established that the DNA remains in a duplex in 1:1 (v/v) mixtures of glycol and various buffers at room temperature (Herskovits, 1962; Green & Mahler, 1968). To check this point, we determined the melting curve for a solution of DNA (5×10^{-5} M in phosphate) in our 1:1 buffer–glycol solvent, by monitoring the thermally induced increase in absorbance at 260 nm. In qualitative agreement with the previous melting studies in mixtures of glycol with other buffers (Green & Mahler, 1968; Rahn, 1973), we found that addition of glycol did not substantially reduce the 35–40% hyperchromicity of the DNA, but it did lower the melting temperature (taken as the midpoint of the thermally induced absorbance increase), relative to the pure buffer solvent; we observed a melting temperature of 45 °C, as compared to 68 °C in buffer alone.

The pyridine samples were prepared by a cryogenic Bridgman technique (Leung, 1974), producing either an extensively cracked glassy or crystalline sample, by lowering the sample in a quartz capillary (i.d. 3 mm) through a sharp temperature gradient (room temperature to ca. 80 K) at a rate of ca. 0.2 cm/h. This was necessary as the pyridine samples prepared by quick freezing produced powdery crystallites and yielded no ODMR spectra, most probably due to increased rates of spin–lattice relaxation. A similar morphology dependence has been observed for pyrazine in a glassy and polycrystalline cyclohexane matrix (Hall & El-Sayed, 1975). We also discounted the possibility that the BePD and BaPT were substantially "zone melted" out of the pyridine matrix, as we noted no change in the chromophore phosphorescence along the length of the sample.

Phosphorescence and ODMR. The methods used for determining 77 K phosphorescence spectra and 2 K ODMR spectra (run at the appropriate phosphorescence maxima) have been described in detail (Lefkowitz et al., 1979). Phosphorescence decays at 77 K were measured by using right angle excitation with synchronously linked shutters for excitation and emission. As all samples exhibited extraneous phosphorescence at the wavelengths of interest, the decay rate of the adduct was derived from the total decay by a generalized least-squares fitting program, using a biexponential fit. The extraneous emission did not contribute to the ODMR spectra, as there was no response to microwave radiation of the phosphorescence at wavelengths away from the pyrene-like peaks.

No D–E signals were noted for any of the compounds in any solvents, even though, as shown later in the paper, the total decay rate differences between x and z sublevels are substantial. Neither MIDP (see below) nor EELDOR [saturating the $2E$ transition while sweeping the D–E spectrum (Leung & El-Sayed, 1972)] was successful in detecting this transition.

Sublevel kinetics were analyzed by using a combination of techniques on the $D + E$ and $2E$ transitions. Slowly decaying sublevel rates were obtained by microwave-induced delayed phosphorescence (MIDP) (Schmidt et al., 1971), which is essentially a 2 K phosphorescence decay measurement where, after waiting some time after the excitation has been extinguished (t_0), the sublevel transition is quickly swept, producing an increase in the phosphorescence intensity (h). If t_0 is sufficiently long to allow the faster of the two sublevels to empty, h will be proportional to the remaining population in the slow sublevel, and the slope of a plot of ln h vs. t_0 will yield that sublevel's total decay rate. In these experiments, the microwave sweeps spanned ca. 100 MHz in 10 ms, employing ca. 1-W power, while phosphorescence decays were cycled for ca. 4 s. Since during the course of all cryogenic experiments there was a substantial attenuation of the phosphorescence intensity, most likely caused by a two photon triplet–triplet absorption to a reactive upper triplet state (Michl & Kok, 1970), the decay curves and h values were normalized to consistent initial phosphorescence intensities.

MIDP experiments on the $D + E$ and $2E$ transitions yielded k_x and k_z, respectively (Figure 2b), and suggested k_y as the "fast" sublevel in both transitions. To extract k_y, we used the microwave fast passage technique (Winscom & Maki, 1971), where, while viewing the steady-state phosphorescence intensity, a fast microwave sweep, similar to that employed in the MIDP experiments, causes an increase in the phosphorescence intensity which decays back to the steady-state value according to

$$\Delta I_{\text{phos}} = A \exp(-k_i t) - B \exp(-k_j t)$$

where A and B are positive quantities, t is the time after the microwave pulse, k_i is the "fast" sublevel total decay rate, and k_j is the slow sublevel decay rate. Due to rather low signal to noise ratios, we could fit the experimental decays to the above function only by fixing k_j at the value obtained from the MIDP experiment. While, as can be seen from Figure 2, k_y can be obtained from either ODMR transition, the values given in the text refer to the stronger $D + E$ transition, though all were found to agree with the values obtained from the $2E$

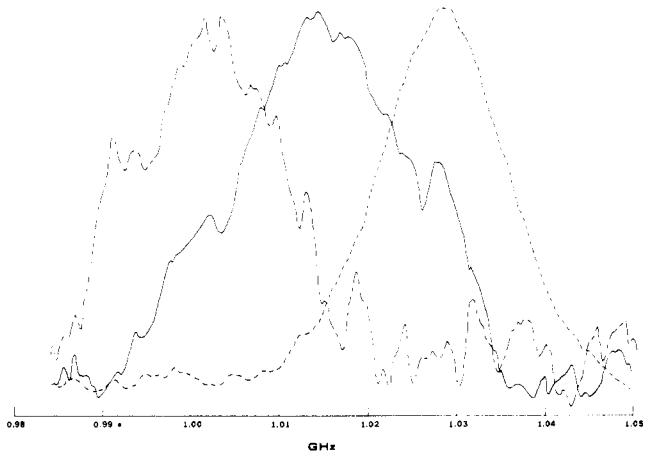

FIGURE 3: $D + E$ ODMR spectra of BePD in pyridine (---), BePD in EGB (---), and BePE–DNA in EGB (—).

transition.

Results and Discussion

BePE–DNA Adduct. In order to model environmental effects on the triplet state chromophore, we have chosen BePD, which is identical with the BePE adduct structure, except for the substitution of a hydroxyl group for the nucleic acid at the BeP carbon 9 position (Figure 1b). BePD is conveniently prepared by hydrolysis of BePE and is more chemically stable than BePE in aqueous media. Furthermore, preliminary experiments on BePE in organic solvents showed its unsuitability as a model system since its phosphorescence and ODMR are very different from either BePD or the DNA adduct, possibly due to the epoxide-induced strain being transmitted to the chromophore.

Dry pyridine was used to model the hydrophobic, heteroaromatic nature of the surroundings expected for an intercalated species, while EGB represents the bulk solvent interactions anticipated for a solvent-exposed chromophore.

The 77 K phosphorescence spectra of the BePE–DNA adduct, BePD in EGB, and BePD in pyridine were very similar, all showing a sharp peak at 581 nm with longer wavelength structure typical of a pyrene-like chromophore (Clar & Zander, 1956). There are, however, substantial differences among the $D + E$ ODMR spectra of these compounds (Figure 3); the BePE–DNA adduct resonance occurs *between* that of the BePD in EGB and pyridine and is significantly broadened with small but reproducible (by reverse microwave sweeping) shoulders on both sides at approximately the same frequencies as the BePD in the two model solvents. This suggests that, on the average, the chromophore in the adduct experiences an intermediate degree of sublevel perturbation, between that expected for complete intercalation and solvent exposure. Moreover, it also indicates that this perturbation is quite heterogeneous, with the ODMR resonances of some adduct chromophores near the "extreme" environment cases modeled by BePD in the two solvents.

The $2E$ ODMR spectra (Figure 4) show similar shifts and broadening in the DNA adduct, though no $2E$ signal for BePD in pyridine was obtained after extensive averaging. These allow the determination of D and E yielding (in GHz) for the adduct $D = 2.061 \pm 0.004$ and $E = -1.046 \pm 0.004$, and for the diol in EGB $D = 2.085 \pm 0.004$ and $E = -1.054 \pm 0.004$. The decrease in D suggests that the pyrene chromophore is more distorted from planarity in the adduct than in the diol in the same solvent, while the smaller change in E indicates that this

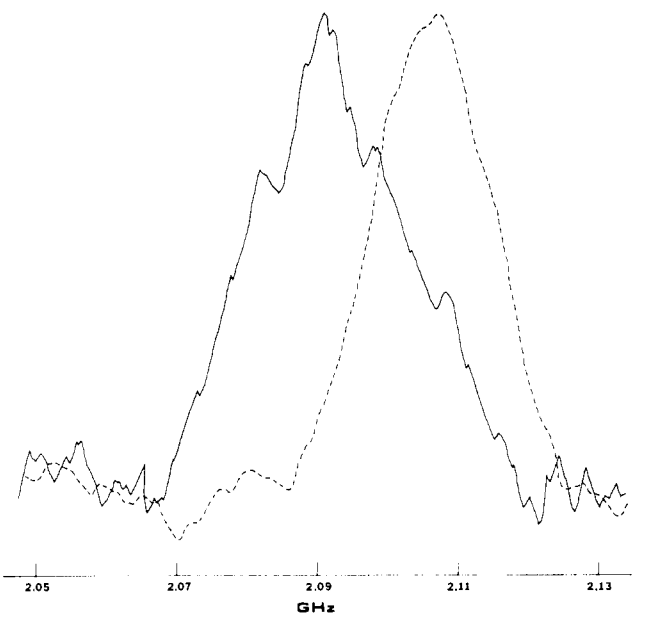

FIGURE 4: $2E$ ODMR spectra of BePE–DNA in EGB (—) and BePD in EGB (---).

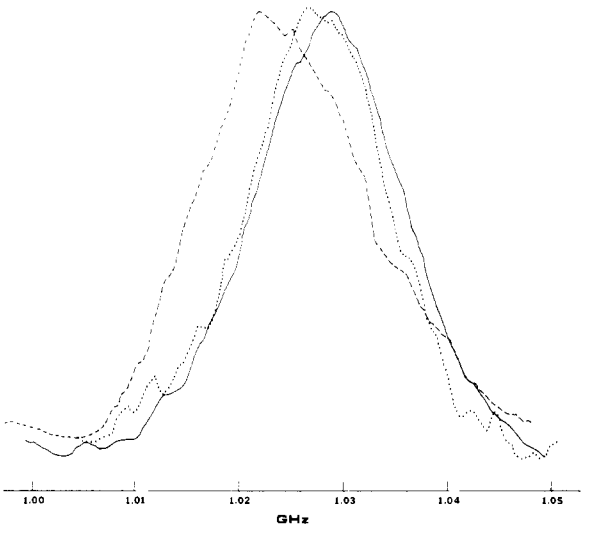

FIGURE 5: $D + E$ ODMR spectra in EGB of BePE–DNA, denatured (---), BePE–DNA, enzymatically digested (···), and BePD (—).

distortion does not significantly alter the spin density differences between the yz and xz molecular planes (see Figure 2a) (El-Sayed, 1970).

To more precisely ascertain the origin of the ODMR frequency line shift and broadening found in the BePE–DNA adduct, we disrupted the nucleic acid double-helical structure by denaturation, producing randomly coiled single strands, and by enzymatically digesting the DNA, yielding single deoxyribonucleoside–BePE adducts. The 77 K phosphorescence spectra of these samples in EGB were not detectably different from that of the "native" DNA adduct, with respect to either peak wavelengths or shapes. The $D + E$ and $2E$ ODMR spectra (Figures 5 and 6, respectively) show that upon denaturation, the adduct ODMR peaks narrow substantially and move closer in frequency to the BePD in EGB spectra, while the digest spectra continue this trend to a lesser degree and very nearly resemble those of the freely solvent exposed model.

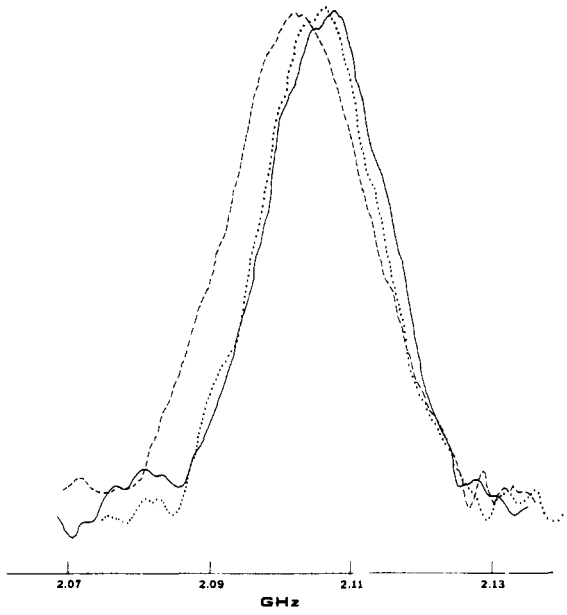

FIGURE 6: 2*E* ODMR spectra in EGB of BePE–DNA, denatured (---), BePE–DNA, enzymatically digested (···), and BePD (—).

These data point to the double-helical structure of the nucleic acid as the predominant source of spectral perturbation of the BePE–DNA adduct's triplet sublevels and are consistent with a conformation where the chromophore resides at least partially in a quasi-intercalative environment.

The remaining differences between the denatured adduct and digest spectra most likely arise from the residual base-stacking interactions present in denatured DNA (Bloomfield et al., 1974), though we have not ruled out the possibility that at least part of this remaining perturbation is caused by the presence of the phosphate groups in the denatured sample, as this moiety has been implicated as a source of ODMR spectral changes in the tryptophan triplet sublevels of proteins with prosthetic phosphate groups (Ross et al., 1980).

A second important conclusion drawn from these results is that ODMR is *not* obviously sensitive to substitutions on the BeP carbon 9 position. As previously noted, BePE binds to DNA with a significant number of adenosine adducts, as well as both cis and trans guanosine adducts, and digestion of the modified DNA yields these distinct products (Kinoshita et al., 1982). However, the digest ODMR spectra do not resolve these different species and are not obviously different from the BePD in EGB spectra, where the deoxyribonucleoside is replaced by a hydroxyl group. These different binding conformations may lead to a variety of local chromophore environments in the "native" adduct, however, and thus may be partly responsible for the ODMR line broadening observed in the BePE–DNA spectra.

Finally we wish to stress that while our data indicate that the chromphore is proximate to the interior of the DNA double helix, it does not imply that the adduct's conformation closely resembles a "classical" intercalation complex found with the planar intercalator parallel to the DNA base planes (Lerman, 1964). Indeed, the adduct's ODMR shift is substantially less than that of the "complete intercalation" model system of BePD in pyridine. Our results are thus in agreement with the photophysical measurements mentioned above (Geacintov et al., 1982), where the pyrene chromophore exhibits properties expected for a conformation with an intermediate degree of intercalation.

BaPDE–DNA Adduct. The 77 K phosphorescence spectra of the BaPDE–DNA adduct and the BaPT in EGB showed

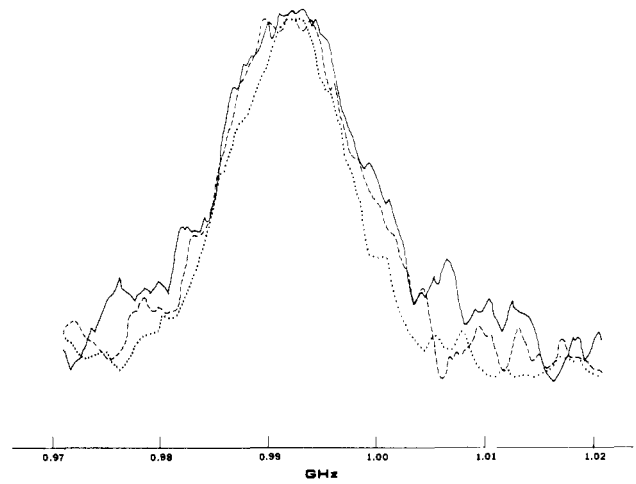

FIGURE 7: $D + E$ ODMR spectra in EGB of BaPDE–DNA, native (—), BaPDE–DNA, denatured (---), and BaPT (···).

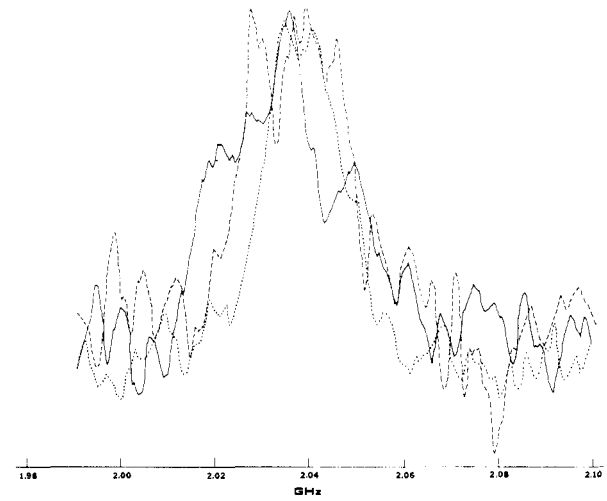

FIGURE 8: 2*E* ODMR spectra in EGB of BaPDE–DNA, native (—), BaPDE–DNA, denatured (---), and BaPT (···).

maxima at 598 nm, while that of BaPT in pyridine was red shifted 4 nm. The $D + E$ ODMR spectra of the native and denatured BaPDE-DNA adducts and of BaPT in EGB (Figure 7) are quite similar, except for a small narrowing of the model system spectrum. The enzymatic digest also exhibits a $D + E$ signal (not shown) nearly identical in frequency and line width with that of the adduct. Also, there are no frequency shifts between the 2*E* spectra (Figure 8) of the tetrol in EGB and the native and denatured DNA adducts, though the native spectrum is somewhat broader and more structured, narrowing a bit upon denaturation. No digest 2*E* spectrum nor either transition for BaPT in pyridine could be detected after extensive signal averaging.

The lack of any large ODMR spectral changes in the BaPDE–DNA adduct emphasizes the lack of nucleic acid induced perturbations on the triplet sublevels, particularly in view of the sublevels' sensitivity toward these interactions, as demonstrated in the BePE adduct. In the BaPDE adduct it thus seems unlikely that the chomophore is "intercalated" into the nucleic acid helix; in any event we may state that any interaction with the nucleic acid is significantly smaller than for the BePE case. We believe that detailed comparisons of both adducts are validated by the similarity of their chromophores, as well as the close analogy between the respective model systems (diol and tetrol) employed. Finally we note that the broadening of the 2*E* transition does demonstrate the

Table I: Sublevel Kinetic Analysis[a]

	system			
	BaPDE–DNA/ EGB	BaPT/ EGB	BePE–DNA/ EGB	BePD/ EGB
k_x	1.9 ± 0.2	1.9 ± 0.1	1.0 ± 0.1	1.2 ± 0.1
k_y	3.6 ± 0.2	4.6 ± 0.2	2.6 ± 0.2	2.9 ± 0.2
k_z	1.2 ± 0.3	1.9 ± 0.2	0.5 ± 0.1	0.6 ± 0.1
77 K[b,c]	2.4 ± 0.1	2.6 ± 0.1	1.4 ± 0.1	1.5 ± 0.1
$\Sigma_i k_i/3$[c]	2.2 ± 0.2	2.8 ± 0.2	1.4 ± 0.1	1.6 ± 0.1

[a] Sublevel total decay rates are given in s^{-1}. [b] The total decay rate of the phosphorescence at 77 K. [c] A measure of the accuracy of the total sublevel decay rates is the criterion that the decay rate at 77 K should equal $\Sigma_i k_i/3$, where k_is are the decay rates measured at helium temperatures, assuming that no additional pathways of triplet decay are introduced at the higher temperature.

presence of some heterogeneous perturbation in the BaPDE–DNA adduct, while the absence of this effect on the $D + E$ peaks indicates that the x sublevel is being preferentially broadened (see Figure 2b).

Sublevel Kinetic Analysis. Since the decay mechanisms for the individual triplet sublevels arise from the same symmetry considerations that help determine the sublevel splittings, we expect both to be environmentally sensitive. As such, we measured the sublevel total decay rates for the BaPDE and BePE adducts and their respective model compounds in EGB. Table I shows that while there is a substantial difference between the BaPDE and BePE systems, there are no clear distinctions between the adduct and model compound, particularly in the BePE system where the ODMR spectra reveal significant nucleic acid–chromophore interactions. We also noted no anomalous enhancements in k_z for either adduct, which have been found for several PAHs physically intercalated into DNA (Chiha et al., 1977, 1978). While this may suggest that neither chromophore is truly intercalated into the DNA helix, other investigators have not found a marked environmental dependence of k_z in other PAHs (Brauchle et al., 1980).

In summary, while we found no clear trends in the sublevel kinetic analysis, this need not imply that the total sublevel decay rates are intrinsically insensitive to the environment, but may only manifest the relatively low precision of the measurements as compared to the sublevel determinations: ca. 10% for the decay rates vs. ca. 0.1% for the sublevel splittings.

Summary and Conclusions

We have presented ODMR evidence indicating that the pyrene-like chromophore in the BePE–DNA adduct exists in a heterogeneous environment, with the primary source of the spectral perturbations being the double-helical structure of the nucleic acid, while the BaPDE adduct spectra are essentially free of DNA induced changes, suggesting that the chromophore resides in an environment quite similar to the bulk solvent. The data, particularly the results of denaturation and digestion, strongly indicate some "quasi-intercalative" geometry for the BePE adduct and emphasize the absence of any intercalative contributions to the ODMR spectra in the BaPDE-modified DNA.

By contrast, Hogan has recently suggested that the pyrene chromophore in BaPDE-modified double-helical DNA fragments resides exclusively in the interior of the nucleic acid (Hogan et al., 1981) and further suggests that any results indicative of a solvent-exposed model external to the nucleic acid helix are artifacts induced by the presence of denatured DNA fragments, which are preferentially modified by the BaPDE. It is immediately apparent that this is *not* the situation for the BePE adduct, since subjecting this sample to denaturing conditions led to large ODMR spectral changes, which would not be expected if the adducts were originally bound to denatured nucleic acid segments. We also believe it unlikely that our BaPDE adducts were exclusively bound to denatured nucleic acid segments, as the DNA solutions used to prepare these adducts exhibited hyperchromicities of ca. 40% (V. Ibanez, personal communication), indicating no significant amounts of denatured nucleic acid. Hence, we expect a substantial number of adducts bound to double-stranded DNA regions. Since the ODMR results show no discernible amounts of BaPDE adducts in intercalative environments, and we estimate (from signal to noise considerations) that we could detect any ODMR signals ca. 10 times less intense than those reported here, it seems that the adducts bound to native DNA segments do reside in a solventlike environment, external to the double helix.

A more general conclusion of this study is that ODMR is a sensitive probe of the local environment of pyrene-like excited triplet chromophores and can reveal important information missing from the conventional phosphorescence spectrum. We are currently applying this tool to structural studies of other covalent adducts with extant pyrene moieties, with the goal of helping elucidate the role played by the structure of the reactive intermediate in the conformation of the nucleic acid adduct.

Acknowledgments

We most gratefully acknowledge the assistance of Dr. Ronald G. Harvey and Dr. H. Mee-Lee for their gifts of BaPDE and BePE, Dr. Victor Ibanez for preparing samples, Dr. Alan Jeffrey for his preparations of the digests and their chromatographic analyses, Kenneth Bell for his help with computer analyses, Vassily Kolubayev for his measurements of DNA melting curves, and Professor N. E. Geacintov for his many stimulating discussions, for providing us with unpublished results, and for his critique of the manuscript.

References

Autrup, H., Harris, C. C., Trump, B. F., & Jeffrey, A. M. (1978) *Cancer Res. 38*, 3689.

Bloomfield V. A., Crothers, D. M., & Tinoco, I., Jr. (1974) *Physical Chemistry of Nucleic Acids*, pp 132–135, Harper and Row, New York.

Brauchle, Chr., Deeg, F. W., & Voitlander, J. (1980) *Chem. Phys. 53*, 373.

Brown, H. S., Jeffrey, A. M., & Weinstein, I. B. (1979) *Cancer Res. 39*, 1673.

Charles, S. W., Fischer, P. H. H., & McDowell, C. A. (1965) *Mol. Phys. 9*, 517.

Chiha, P. A., Clarke, R. H., & Kramer, E. (1977) *Chem. Phys. Lett. 50*, 61.

Chiha, P. A., Clarke, R. H., Kramer, E., & Lasser, N. (1978) *Semicond. Insul. 4*, 377.

Clar, E., & Zander, M. (1956) *Chem. Ber. 89*, 749.

Drinkwater, N. R., Miller, J. A., Miller, E. C., & Yang, N. C. (1978) *Cancer Res. 38*, 3247.

El-Sayed, M. A. (1970) *Pure Appl. Chem. 24*, 475.

Geacintov, N. E., Gagliano, A., Ivanovic, V., & Weinstein, I. B. (1978) *Biochemistry 17*, 5256.

Geacintov, N. E., Gagliano, A. G., Ibanez, V., & Harvey, R. G. (1982) *Carcinogenesis (London) 3*, 247.

Gordon, A. J., & Ford, R. A. (1972) *The Chemist's Companion*, pp 428–437, Wiley, New York.

Green, G., & Mahler, H. R. (1968) *Biopolymers 6*, 1509.

Hall, L. H., & El-Sayed, M. A. (1975) *Chem. Phys. 8*, 272.

Harvey, R. G., & Fu, P. P. (1978) in *Polycyclic Hydrocarbons and Cancer* (Gelboin, H. V., & Ts'o, P. O. P., Eds.) Vol. 1, pp 133–165, Academic Press, New York.
Herskovits, T. T. (1962) *Arch. Biochem. Biophys. 97*, 474.
Hogan, M. E., Dattagupta, N., & Whitlock, J. P., Jr. (1981) *J. Biol. Chem. 256*, 4504.
Jeffrey, A. M., Weinstein, I. B., Jennette, K. W., Grzeskowiak, K., Nakanishi, K., Harvey, R. G., Autrup, H., & Harris, C. (1977) *Nature (London) 269*, 348.
Kinoshita, T. K., Lee, H. M., Harvey, R. G., & Jeffrey, A. M. (1982) *Carcinogenesis (London) 3*, 255.
Kwiram, A. L. (1972) *MTP Int. Rev. Sci.: Magn. Reson., Ser. One 4*, 271–316.
Lefkowitz, S. M., & Brenner, H. C. (1981) *J. Am. Chem. Soc. 103*, 5257.
Lefkowitz, S. M., Brenner, H. C., Astorian, D. G., & Clarke, R. H. (1979) *FEBS Lett. 105*, 77.
Lerman, L. S. (1964) *J. Mol. Biol. 10*, 367.
Leung, M. (1974) Ph.D Thesis, University of California, Los Angeles, CA.
Leung, M., & El-Sayed, M. A. (1972) *Chem. Phys. Lett. 16*, 454.
MacLeod, M. C., Cohen, G. M., & Selkirk, J. K. (1979) *Cancer Res. 39*, 3463.
Michl, J., & Kok, J. (1970) *J. Am. Chem. Soc. 92*, 4148.
Miller, J. A. (1970) *Cancer Res. 30*, 559.
Nelson, R. G., & Johnson, W. C. (1970) *Biochem. Biophys. Res. Commun. 41*, 211.
Prusik, T., Geacintov, N. E., Tobiasz, C., Ivanovic, V., & Weinstein, I. B. (1979) *Photochem. Photobiol. 29*, 223.
Rahn, R. O. (1973) *Photophysiology 8*, 231.
Ross, J. B., Rousslang, K. W., & Kwiram, A. L. (1980) *Biochemistry 19*, 876.
Schmidt, J., Antheunis, D. A., & van der Waals, J. H. (1971) *Mol. Phys. 22*, 1.
Sims, P., Grover, P. L., Swaisland, A., Pal, K., & Hewer, A. (1974) *Nature (London) 252*, 326.
Weinstein, I. B., Jeffrey, A. M., Jennette, A. W., Blobstein, S. H., Harvey, R. G., Harris, C., Autrup, H., Kasai, H., & Nakanishi, K. (1976) *Science (Washington, D.C.) 193*, 592.
Weinstein, I. B., Jeffrey, A. M., Leffler, S., Pulkrabek, P., Yamasaki, H., & Grunberger, D. (1978) in *Polycyclic Hydrocarbons and Cancer* (Gelboin, H. V., & Ts'O, P. O. P., Eds.) Vol. 2, pp 4–30, Academic Press, New York.
Winscom, C. J., & Maki, A. H. (1971) *Chem. Phys. Lett. 12*, 264.
Wood, A. W., Levin, W., Thakker, D. R., Yagi, H., Chang, R. L., Ryan, D. E., Thomas, P. E., Dansette, P. M., Whittaker, N., Turujman, S., Lehr, R. E., Kumar, S., Jerina, D. M., & Conney, A. H. (1979) *J. Biol. Chem. 254*, 4408.
Wood, A. W., Chang, R. L., Huang, M. T., Levin, W., Lehr, R. E., Kumar, S., Thakker, D. R., Yagi, H., Jerina, D. M., & Conney, A. H. (1980) *Cancer Res. 40*, 1985.

Pumpkin Seed Inhibitor of Human Factor XII_a (Activated Hageman Factor) and Bovine Trypsin†

Yoshio Hojima,‡ Jack V. Pierce, and John J. Pisano*

ABSTRACT: A strong inhibitor of human Hageman factor fragment (HF_f, β-factor XII_a) and bovine trypsin was isolated from pumpkin (*Cucurbita maxima*) seed extracts by acetone fractionation, by chromatography on columns of diethylaminoethylcellulose and carboxylmethyl-Sephadex C-25, and by Sephadex G-50 gel filtration. Pumpkin seed Hageman factor inhibitor (PHFI) is unusual in its lack of inhibition of several other serine proteinases tested—human plasma, human urinary, and porcine pancreatic kallikreins, human α-thrombin, and bovine α-chymotrypsin. Human plasmin and bovine factor X_a are only weakly inhibited. PHFI also inhibits the HF_f-dependent activation of plasma prekallikrein and clotting of plasma. Other properties of PHFI are a p*I* of 8.3, 29 amino acid residues, amino-terminal arginine, carboxyl-terminal glycine, 3 cystine residues, undetectable sulfhydryl groups and carbohydrate, and arginine at the reactive site. The minimum molecular weight of PHFI is 3268 by amino acid analysis. PHFI may be the smallest protein inhibitor of trypsin known.

In the course of screening plant materials for serine proteinase inhibitors, especially for inhibitors of Hageman factor fragment (HF_f, β-factor XII_a)[1] and the kallikreins, we found that corn extracts contain a highly specific HF_f inhibitor (Hojima et al., 1980a). Certain other seeds and especially flower bulbs are extraordinarily rich sources of inhibitors with a variety of specificities (Hojima et al., 1980b). Of these, pumpkin seed extracts are noteworthy because they contain an unusually low molecular weight trypsin inhibitor that strongly inhibits HF_f but does not inhibit plasma kallikrein. We now report the

† From the Section on Physiological Chemistry, Laboratory of Chemistry, National Heart, Lung, and Blood Institute, National Institutes of Health, Bethesda, Maryland 20205. *Received June 22, 1981; revised manuscript received October 6, 1981.*

‡ Present address: Department of Immunopathology, Scripps Clinic and Research Foundation, La Jolla, CA 92037.

[1] Abbreviations: HF_f, Hageman factor fragment (β-factor XII_a); PHFI, pumpkin HF_f inhibitor; PCPI, potato carboxypeptidase inhibitor; PTI, basic pancreatic trypsin inhibitor (Kunitz); BSA, bovine serum albumin; *p*NA, *p*-nitroanilide; Bz, benzoyl; Pip, L-pipecolyl; Tos, tosyl; OMe, methyl ester; OEt, ethyl ester; Z, carbobenzoxy; SBzl, thiobenzyl ester; IU, inhibitor unit; $NaDodSO_4$, sodium dodecyl sulfate; CM, carboxymethyl; DEAE, diethylaminoethyl. Common abbreviations for amino acid residues are used; all are of the L configuration unless otherwise indicated.